

УДК 543.42

Ü. HALDNA, R. A. COX, R. JUGA, E. RAJAVEE

## ESTIMATION OF IONS CONCENTRATION IN AQUEOUS SULFURIC ACID MIXTURES BY RESOLUTION OF RAMAN SPECTRA

(Presented by O. Eisen)

The ionic composition of aqueous sulfuric acid solutions has mostly been studied by Raman spectroscopy [1-3]. The majority of researchers have accepted the respective results obtained by H. Chen and D. E. Irish [1]. The concentration profiles of  $\text{SO}_4^{2-}$  and  $\text{HSO}_4^-$  presented in [1] have been used for the calculation of the hydrated proton concentration [4] ( $C_{\text{H}^+} = C_{\text{Hso}_4^-} + 2C_{\text{so}_4^{2-}}$ ). The last quantity ( $C_{\text{H}^+}$ ), in turn, plays an important role in determining weak bases basicity constants by the excess acidity method [4]. It should be noted that H. Chen and D. E. Irish [1] discussed the existence of ion pairs  $\text{H}_3\text{O}^+ \cdot \text{SO}_4^{2-}$  and  $\text{H}_3\text{O}^+ \cdot \text{HSO}_4^-$ , but no attempt was made to estimate their concentrations separately from those of the respective nonionpaired species. In recent years, some evidence has been accumulated showing that in the system  $\text{H}_2\text{SO}_4 - \text{H}_2\text{O}$  both ions,  $\text{SO}_4^{2-}$  and  $\text{HSO}_4^-$ , may exist as free ions and as ion pairs [2, 3, 5, 6, 7]. The structure of the latter has been discussed by several authors [5-7]. In the present paper free ions are denoted as  $\text{HSO}_4\text{AQ}$ ,  $\text{SO}_4\text{AQ}$  and ionpaired ones as  $\text{HSO}_4\text{IP}$ ,  $\text{SO}_4\text{IP}$ , respectively.

H. Chen and D. E. Irish [1] measured the Raman spectra of aqueous sulfuric acid solutions in the range of 2.52-80.58%  $\text{H}_2\text{SO}_4$  (w/w). In the paper of R. A. Cox et al. [5] the same was done in a wider range, viz. 4.53-99.48%  $\text{H}_2\text{SO}_4$  (w/w). The mathematical treatment of these spectra [5] was carried out using factor analysis (FA) techniques. Two FA methods have been applied to these spectra [5]: the principal component analysis (PCA) [8] and a novel approach — the spectral isolation analysis (SIA) [9]. The application of FA methods has led to a conclusion that the Raman spectra studied may be presented as a sum of three spectral components which may most likely be assigned to the following sums of species ( $\text{SO}_4\text{AQ} + \text{HSO}_4\text{AQ}$ ), ( $\text{SO}_4\text{IP} + \text{HSO}_4\text{IP}$ ) and ( $\text{H}_2\text{SO}_4$ ) [5, 6]. The latter is the undissociated sulfuric acid detected in concentrated  $\text{H}_2\text{SO}_4$  solutions. The individual concentration profiles for the species involved were not obtained by the FA methods applied [5, 6]. Nevertheless, PCA [8] followed by the curve-fitting procedures yielded the number of individual but overlapping bands in the spectra studied [5]. Altogether 18 spectral bands were resolved out and their maximum locations determined [5]. This information has been used in the present study in order to obtain concentration profiles for the species present in aqueous sulfuric acid solutions.

### Raman spectra and their resolution into bands

The set of spectra used was the same as in [5, 6]. It consists of 25 Raman spectra covering the range of 4.53-96.71%  $\text{H}_2\text{SO}_4$  (w/w). The experimental part has been published elsewhere [5]. The intensities of spectra

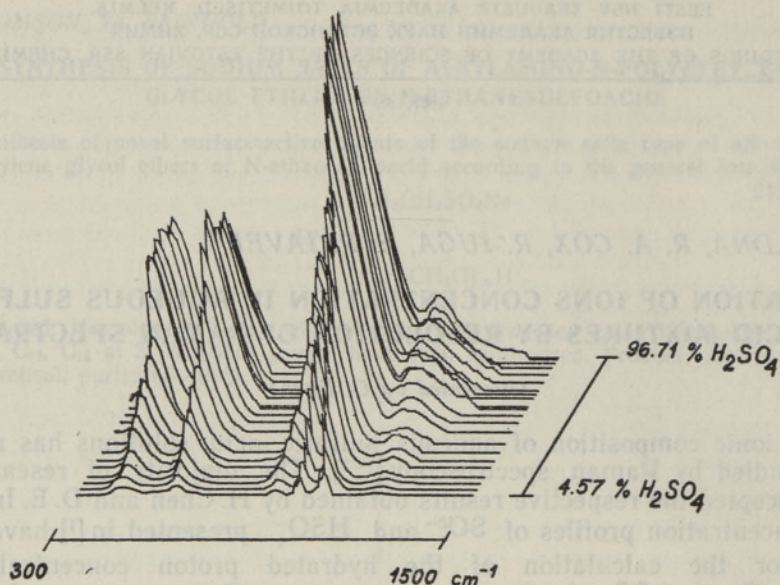


Fig. 1. Standardized Raman spectra of water sulfuric acid mixtures.

were corrected for laser power and signal amplification taking the spectrum of a standard solution (in our case 36.74%  $\text{H}_2\text{SO}_4$  w/w) before and after each spectrum studied [10]. A factor ( $H$ ) equal to the mean intensity of the standard solution at  $1035\text{ cm}^{-1}$  taken before and after the spectrum studied was calculated. The standardized intensities  $I(\nu)$  of the spectra studied were obtained according to the equation [10, 11]

$$I(\nu) = I(\nu)_{\text{obs}} / [H \cdot (\nu - \nu_1)^4], \quad (1)$$

where  $\nu$  is the wavenumber ( $\text{cm}^{-1}$ ) for the observed intensity  $I(\nu)_{\text{obs}}$  and  $\nu_1$  is the wavenumber of the laser line used ( $20485\text{ cm}^{-1}$  in our case corresponding to the 488 nm line of the argon ion laser). The spectra in analog form were digitalized by hand taking the intensity readings in  $10\text{ cm}^{-1}$  steps along the  $\nu$ -axis. Each recorded band on spectra has been described by 10–15 points ( $10\text{ cm}^{-1}$  apart from each other). This seems to be sufficient for fixing the bands shape unambiguously. The intensity readings were taken from the baseline constructed by hand using “empty” spectral regions. The intensities were digitalized in the range of  $300\text{--}1500\text{ cm}^{-1}$  at the same wavenumbers on each spectrum. In this way a spectral data array of  $25 \times 120$  points was obtained. Fig. 1 shows the standardized spectra. The relative intensities  $I(\nu)_{\text{obs}}/H$  for the maximum at  $1030\text{--}1050\text{ cm}^{-1}$  are presented in Table 1. Each spectrum was curve-fitted as a sum of Voigt profiles [12, 13] which are Gaussian–Lorentzian convolutions. Following S. Ikawa and M. Kimura [12] we have used Kielkopf’s approximation to the Voigt profile [14] with the additional assumption that the Gaussian part of the profile comes only from the finite slit width,  $5\text{ cm}^{-1}$  in our case, i. e. each peak has a Gaussian half-width [5, 13] of  $3.0\text{ cm}^{-1}$ . Consequently, each Raman band can be specified by one fixed ( $\beta_G$ ) and three adjustable ( $h$ ,  $\beta_L$ ,  $\nu_{\text{max}}$ ) parameters ( $h$  is the intensity of the band at its maximum  $\nu_{\text{max}}$  and  $\beta_G$ ,  $\beta_L$  are half-widths for the Gaussian and Lorentzian part, respectively). The values of  $\nu_{\text{max}}$  from [5] (see Table 2) were used in the iteration procedures as zero approximations. Two bands out of the 18 resolved out in [5] were not used by us (viz. those at  $729\text{ cm}^{-1}$  assigned to  $\text{H}_2\text{SO}_4$ , because it is too weak [5, 6], and a band

Table 1

Relative intensity of the maximum at 1030–1050  $\text{cm}^{-1}$ 

| $\% \text{H}_2\text{SO}_4$ | $I_{\text{obs}}(\nu)/H$ | $\% \text{H}_2\text{SO}_4$ | $I_{\text{obs}}(\nu)/H$ |
|----------------------------|-------------------------|----------------------------|-------------------------|
| 4.57                       | 15                      | 65.26                      | 152                     |
| 8.05                       | 26                      | 67.72                      | 155                     |
| 11.78                      | 41                      | 69.96                      | 158                     |
| 15.86                      | 52                      | 75.05                      | 162                     |
| 21.90                      | 70                      | 80.10                      | 159                     |
| 23.86                      | 80                      | 84.26                      | 149                     |
| 31.19                      | 89                      | 87.42                      | 136                     |
| 36.74                      | 101                     | 89.58                      | 125                     |
| 44.02                      | 112                     | 90.63                      | 120                     |
| 50.03                      | 128                     | 92.09                      | 114                     |
| 54.40                      | 136                     | 94.29                      | 105                     |
| 58.49                      | 142                     | 96.71                      | 99                      |
| 59.88                      | 144                     |                            |                         |

at  $590 \text{ cm}^{-1}$  assigned to  $\text{HSO}_4\text{IP}$  as it is too close to the band at  $595 \text{ cm}^{-1}$ ). As a result, at  $595 \text{ cm}^{-1}$  a complex band was resolved out and assigned to  $\text{SO}_4\text{AQ}$ ,  $\text{HSO}_4\text{AQ}$ ,  $\text{HSO}_4\text{IP}$  [5]. This band as well as those at  $433$  and  $1200 \text{ cm}^{-1}$  were further not used to calculate species concentration due to their complex assignments (see Table 2).

Table 2

The spectral bands used in curve-fitting procedures

| N  | $\nu_{\text{max}}$ | Assignment  | $A^*_{\text{max}}$ |
|----|--------------------|---|--------------------|
| 1  | 1361               | $\text{H}_2\text{SO}_4$   | 1.8                |
| 2  | 1200               | $\text{H}_2\text{SO}_4$ , $\text{HSO}_4\text{AQ}$ , $\text{HSO}_4\text{IP}$ | 12.6               |
| 3  | 1147               | $\text{H}_2\text{SO}_4$   | 25.6               |
| 4  | 1103               | $\text{SO}_4\text{AQ}$  | 0.3                |
| 5  | 1055               | $\text{HSO}_4\text{AQ}$   | 8.8                |
| 6  | 1037               | $\text{HSO}_4\text{IP}$   | 38.8               |
| 7  | 987                | $\text{SO}_4\text{AQ}$  | 12.7               |
| 8  | 935                | $\text{SO}_4\text{IP}$  | 3.0                |
| 9  | 918                | $\text{H}_2\text{SO}_4$   | 15.2               |
| 10 | 899                | $\text{HSO}_4\text{IP}$   | 20.0               |
| 11 | 877                | $\text{HSO}_4\text{AQ}$   | 1.3                |
| 12 | 595                | $\text{SO}_4\text{AQ}$ , $\text{HSO}_4\text{AQ}$ , $\text{HSO}_4\text{IP}$  | 17.2               |
| 13 | 563                | $\text{H}_2\text{SO}_4$   | 27.2               |
| 14 | 433                | $\text{H}_2\text{SO}_4$ , $\text{SO}_4\text{AQ}$ , $\text{HSO}_4\text{AQ}$  | 19.8               |
| 15 | 417                | $\text{HSO}_4\text{IP}$   | 4.7                |
| 16 | 395                | $\text{H}_2\text{SO}_4$   | 2.4                |

\* Max. values of area in relative but comparable between themselves units.

A program in FORTRAN IV including the standard least-squares curve-fitting subroutine [15] was written which yields optimum values for  $\beta_L$ ,  $\nu_{\text{max}}$  and  $h$ . Computations were performed on an EC 1052 computer, Institute of Cybernetics, Estonian SSR Academy of Sciences. It should be noted that there exists an "empty" spectral region between  $700$ – $800 \text{ cm}^{-1}$ . This was used to carry out the curve-fitting procedures for the bands  $\nu_{\text{max}} > 800 \text{ cm}^{-1}$  and  $\nu_{\text{max}} < 700 \text{ cm}^{-1}$  separately. In the range of  $1500$ – $800 \text{ cm}^{-1}$  11 bands (the respective maxima at  $1361$ ,  $1200$ ,  $1147$ ,  $1103$ ,  $1055$ ,  $1037$ ,  $987$ ,  $935$ ,  $918$ ,  $899$ ,  $877 \text{ cm}^{-1}$ ) and in the range of  $700$ – $300 \text{ cm}^{-1}$

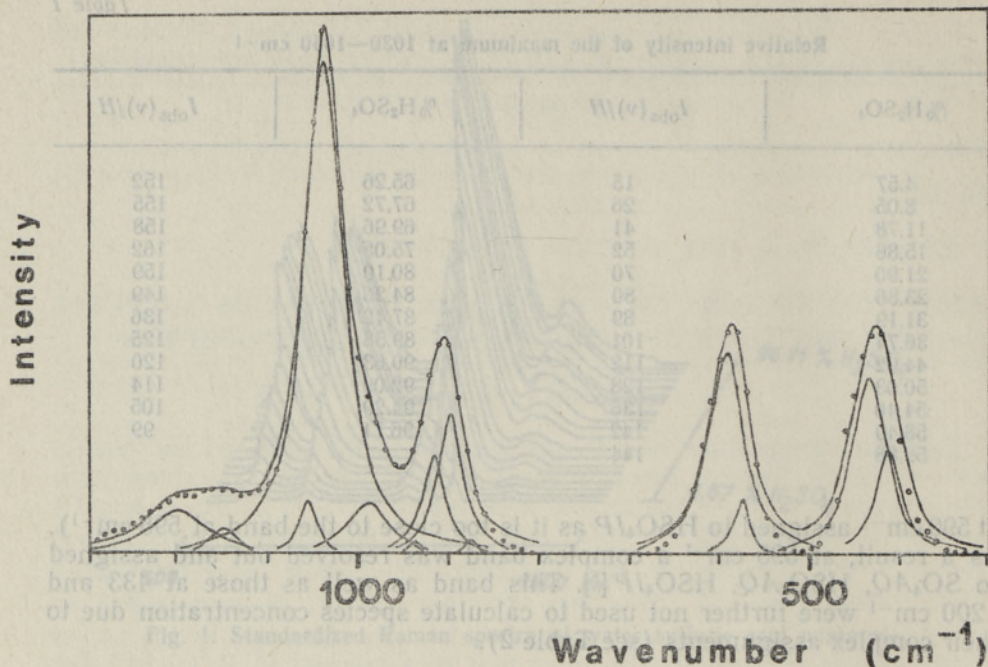


Fig. 2. Experimental spectrum points, resolution bands and calculated spectrum of 75.05% (w/w) aqueous sulfuric acid solution.

Table 3

Areas of peaks ( $A_i$ ) in the Raman spectra of aqueous sulfuric acid solutions. Region 1500—800  $\text{cm}^{-1}$

| %H <sub>2</sub> SO <sub>4</sub> | $A_i^*$ for the peak $\nu_{\text{max}}$ at $\text{cm}^{-1}$ |      |      |      |      |      |      |     |      |      | RA** |     |
|---------------------------------|---|------|------|------|------|------|------|-----|------|------|------|-----|
|                                 | 1360  | 1200 | 1147 | 1103 | 1055 | 1037 | 987  | 935 | 918  | 899  |      | 877 |
| 4.57                            |   | 0.3  |      |      | 1.1  | 0.7  | 1.3  | 0   |      | 0.2  | 0    | 36  |
| 8.05                            |   | 0.3  |      |      | 2.5  | 0.5  | 2.2  | 0   |      | 1.0  | 0    | 31  |
| 11.78                           |   | 0.6  |      |      | 3.8  | 1.1  | 2.8  | 0   |      | 1.2  | 0.5  | 11  |
| 15.86                           |   | 0.6  |      |      | 4.2  | 2.1  | 4.3  | 0.2 |      | 1.8  | 0.3  | 11  |
| 21.90                           |   | 1.4  |      |      | 6.1  | 3.6  | 6.6  | 0.5 |      | 3.0  | 0.1  | 10  |
| 23.86                           |   | 2.1  | 0    |      | 7.2  | 5.6  | 7.6  | 0.8 |      | 3.6  | 0.2  | 7   |
| 31.19                           |   | 3.2  | 0.1  |      | 7.1  | 8.4  | 9.3  | 1.8 |      | 3.6  | 0.5  | 6   |
| 36.74                           |   | 2.6  | 0.2  |      | 7.1  | 10.1 | 11.0 | 2.3 |      | 4.8  | 0.1  | 7   |
| 44.02                           |   | 3.0  | 0.4  |      | 8.8  | 12.5 | 11.9 | 2.6 |      | 5.2  | 0.9  | 5   |
| 50.03                           |   | 3.0  | 0.4  |      | 7.6  | 19.4 | 12.7 | 2.6 | 0    | 6.7  | 1.2  | 4   |
| 54.40                           |   | 4.1  | 0.8  |      | 5.3  | 23.3 | 12.4 | 3.0 | 0.1  | 6.9  | 1.3  | 5   |
| 58.49                           |   | 7.2  | 0.9  |      | 5.6  | 23.4 | 11.2 | 2.2 | 0.4  | 7.0  | 1.2  | 4   |
| 59.88                           |   | 5.0  | 1.3  |      | 3.6  | 26.2 | 11.5 | 2.2 | 1.0  | 7.0  | 1.0  | 5   |
| 65.26                           |   | 5.5  | 1.1  |      | 2.0  | 31.4 | 9.2  | 1.9 | 1.2  | 7.6  | 0.8  | 6   |
| 67.72                           |   | 5.2  | 1.0  | 0    | 2.0  | 33.0 | 7.9  | 1.5 | 1.7  | 8.8  | 0.9  | 5   |
| 69.96                           |   | 5.2  | 1.4  | 0    | 1.5  | 36.7 | 6.5  | 1.2 | 2.0  | 9.0  | 0.2  | 5   |
| 75.05                           |   | 6.1  | 1.3  | 0.3  | 1.4  | 38.2 | 5.7  | 1.3 | 2.5  | 9.0  | 0    | 4   |
| 80.10                           |   | 7.5  | 1.3  | 0.2  | 1.3  | 38.8 | 1.6  | 0.6 | 3.2  | 9.4  |      | 4   |
| 84.26                           | 0   | 7.8  | 2.8  | 0.1  | 0    | 38.5 | 1.2  | 0   | 1.9  | 10.0 |      | 4   |
| 87.42                           | 0   | 6.6  | 5.7  | 0    |      | 38.5 | 0    |     | 3.0  | 11.5 |      | 5   |
| 89.58                           | 0.9   | 9.9  | 8.6  |      |      | 34.8 |      |     | 7.0  | 13.0 |      | 4   |
| 90.63                           | 0.5   | 12.6 | 9.4  |      |      | 37.5 |      |     | 8.4  | 13.5 |      | 5   |
| 92.09                           | 0.8   | 7.3  | 13.7 |      |      | 30.7 |      |     | 7.4  | 14.5 |      | 5   |
| 94.29                           | 1.2   | 7.6  | 21.4 |      |      | 26.5 |      |     | 9.8  | 17.0 |      | 6   |
| 96.71                           | 1.8   | 10.2 | 25.6 |      |      | 20.4 |      |     | 15.2 | 20.0 |      | 11  |

\* The units used — see the subscript to Table 2.

\*\* Ratio RA (Eq. 2).

five peaks (the respective maxima at 595, 563, 433, 417, 395  $\text{cm}^{-1}$ ) were considered. The curve-fitting procedure was performed several times for each spectrum region using different initial values for  $\beta_L$ ,  $\nu_{\max}$  and  $h$  every time. The choice of the initial values for  $\beta_L$  and  $h$  has a minor influence on band area: the relative scatter in band areas was  $<10\%$  of the respective mean value. The areas under the Voigt profiles were obtained by the trapezium method, using  $2 \text{ cm}^{-1}$  steps. The results of the curve-fitting procedure are presented in Tables 3 and 4 (see Fig. 2). The magnitude of the misfit was estimated by the ratio

$$RA = 100 \cdot A_{a,b}^{-1} \cdot \int_a^b |I(\nu)_{\text{obs}} - I(\nu)_{\text{calc}}| d\nu, \quad (2)$$

where  $A_{a,b}$  is the area under the standardized spectrum observed (Eq. 1) in the region  $a \leq \nu \leq b$  and  $I(\nu)_{\text{obs}}$ ,  $I(\nu)_{\text{calc}}$  are the observed (Eq. 1) and calculated intensity values at the wavenumber  $\nu$ , respectively. The  $I(\nu)_{\text{calc}}$  was obtained as a sum of band intensities at the  $\nu$  considered. The values of  $RA$  presented in Tables 3 and 4 demonstrate that the curve-fitting procedure yielded rather good results ( $4\% \leq RA \leq 15\%$ ).

The  $\nu_{\max}$  values found depend on the stoichiometric acid concentration as shown in Fig. 3. Their values at the respective band area maximum are close to those given in Table 2. The dependence of  $\nu_{\max}$  on the sulfuric acid stoichiometric concentration in the case of bands near 1050 and 980  $\text{cm}^{-1}$  has also been found by S. Ikawa [12].

Table 4

Areas of peaks ( $A_i$ ) in the Raman spectra of aqueous sulfuric acid solutions.  
Region 300–700  $\text{cm}^{-1}$

| %H <sub>2</sub> SO <sub>4</sub> | $A_i^*$ for the peak $\nu_{\max}$ at $\text{cm}^{-1}$ |      |      |     |     | RA** |
|---------------------------------|---|------|------|-----|-----|------|
|                                 | 595   | 563  | 433  | 417 | 395 |      |
| 4.57                            | 1.5   |      | 1.4  |     |     | 19   |
| 8.05                            | 1.9   |      | 2.1  |     |     | 15   |
| 11.78                           | 2.7   |      | 2.7  |     |     | 10   |
| 15.86                           | 3.9   |      | 3.5  |     |     | 23   |
| 21.90                           | 6.6   |      | 5.7  |     |     | 18   |
| 23.86                           | 7.1   |      | 6.7  | 0   |     | 13   |
| 31.19                           | 8.0   |      | 8.1  | 0.3 |     | 10   |
| 36.74                           | 8.2   |      | 9.5  | 0.2 |     | 12   |
| 44.02                           | 9.4   |      | 11.5 | 0.2 |     | 20   |
| 50.03                           | 10.6  |      | 10.2 | 2.0 |     | 24   |
| 54.40                           | 14.5  | 0    | 13.1 | 1.6 |     | 11   |
| 58.49                           | 17.2  | 0.2  | 19.8 | 1.2 |     | 15   |
| 59.88                           | 15.0  | 0.2  | 19.0 | 1.5 |     | 15   |
| 65.26                           | 16.6  | 0.6  | 17.0 | 2.5 | 0   | 15   |
| 67.72                           | 16.0  | 0.7  | 16.9 | 2.9 | 0.1 | 15   |
| 69.96                           | 15.6  | 0.6  | 12.5 | 3.2 | 0.1 | 25   |
| 75.05                           | 14.4  | 1.8  | 12.6 | 4.7 | 0.4 | 19   |
| 80.10                           | 13.6  | 3.0  | 11.8 | 4.2 | 0.6 | 16   |
| 84.26                           | 16.1  | 4.7  | 10.1 | 3.4 | 1.3 | 6    |
| 87.42                           | 13.0  | 7.0  | 9.7  | 2.8 | 1.4 | 15   |
| 89.58                           | 10.8  | 13.0 | 11.0 | 3.8 | 1.2 | 11   |
| 90.63                           | 9.8   | 16.2 | 10.0 | 4.6 | 1.3 | 11   |
| 92.09                           | 10.2  | 19.8 | 9.6  | 3.4 | 1.5 | 11   |
| 94.29                           | 11.0  | 22.4 | 10.8 | 1.7 | 1.9 | 9    |
| 96.71                           | 9.7   | 27.2 | 10.6 | 2.5 | 2.4 | 10   |

\* The units used — see the subscript to Table 2.

\*\* Ratio  $RA$  (Eq. 2).

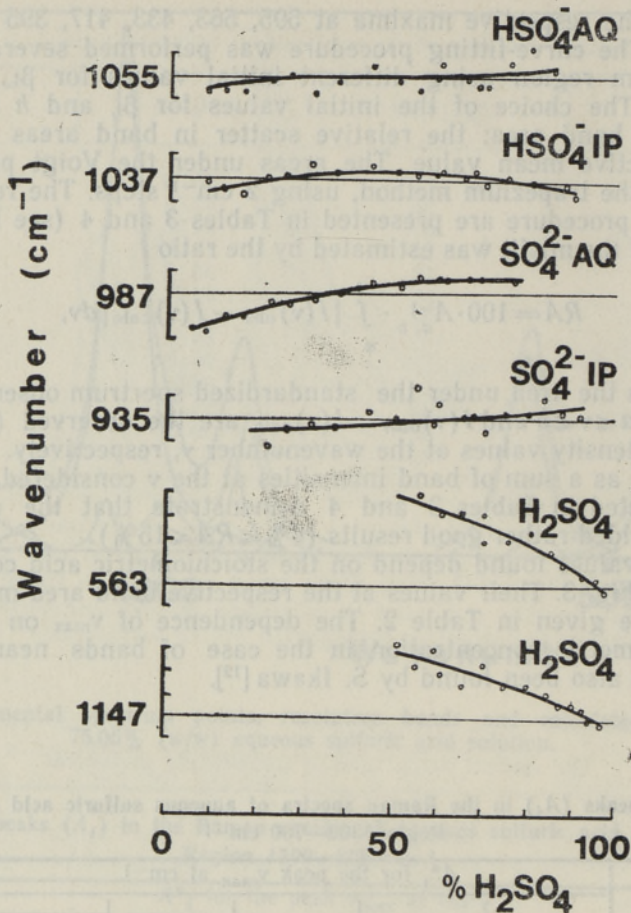


Fig. 3. Dependence of band maximum on stoichiometric acid concentration for the band used. On ordinate axes marks stand for every 5  $\text{cm}^{-1}$ .

### Species concentration in aqueous sulfuric acid mixtures

Raman band area  $A$  is related to the concentration of the species which generates the band through the equation in [10]

$$A = J \cdot C, \quad (3)$$

where  $J$  is the specific or molar intensity of the band, and  $C$  is the scattering species concentration in moles per liter. The areas of all the bands listed in Table 2 were plotted vs. %  $\text{H}_2\text{SO}_4$  (except the bands at 1200, 595 and 433  $\text{cm}^{-1}$  for the reasons mentioned above; the bands at 1361 and 1103  $\text{cm}^{-1}$  were also neglected because of their very small areas). For some bands, mostly rather weak ones at 395, 918  $\text{cm}^{-1}$  (both  $\text{H}_2\text{SO}_4$ ), 877  $\text{cm}^{-1}$  ( $\text{HSO}_4\text{AQ}$ ) and 417, 899  $\text{cm}^{-1}$  ( $\text{HSO}_4\text{IP}$ ) the profiles  $A$  vs. %  $\text{H}_2\text{SO}_4$  (w/w) exhibit quite a remarkable scatter. Therefore these bands were not used for the estimation of species concentrations. After making these exclusions the following bands remained for further treatment: 987  $\text{cm}^{-1}$  ( $\text{SO}_4\text{AQ}$ ), 1055  $\text{cm}^{-1}$  ( $\text{HSO}_4\text{AQ}$ ), 935  $\text{cm}^{-1}$  ( $\text{SO}_4\text{IP}$ ), 1037  $\text{cm}^{-1}$  ( $\text{HSO}_4\text{IP}$ ), 563 and 1147  $\text{cm}^{-1}$  (both for  $\text{H}_2\text{SO}_4$ ). The areas of these bands were standardized according to

$$B = A/A_{\max}, \quad (4)$$

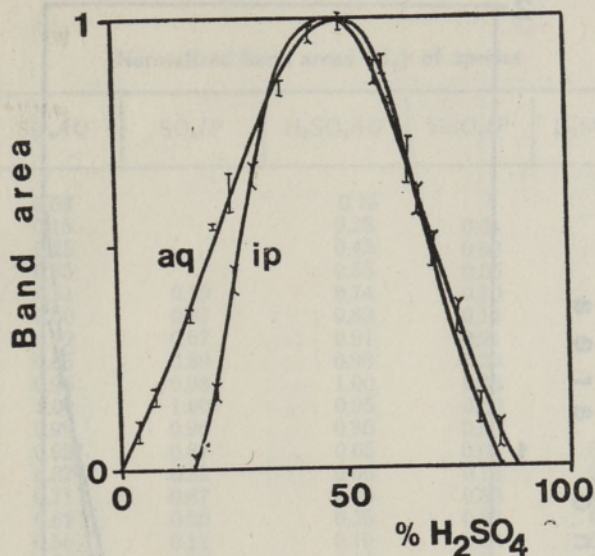


Fig. 4. Normalized areas of the bands specified to  $\text{SO}_4\text{AQ}$  and  $\text{SO}_4\text{IP}$  vs. % (w/w)  $\text{H}_2\text{SO}_4$ . Vertical bars represent uncertainties.

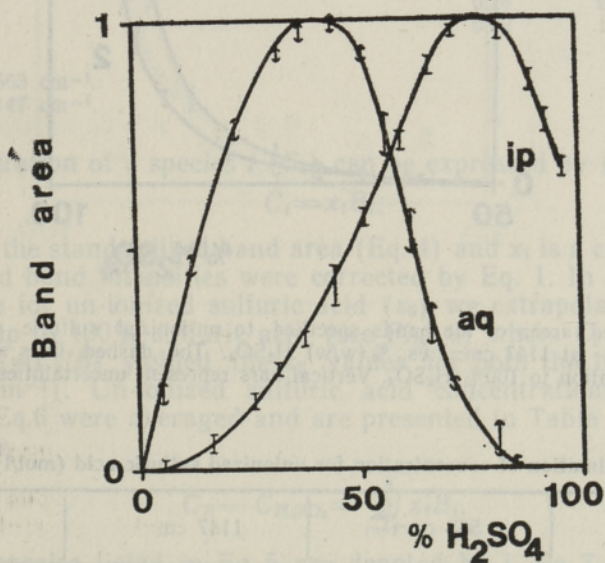


Fig. 5. Normalized areas of the bands specified to  $\text{HSO}_4\text{AQ}$  and  $\text{HSO}_4\text{IP}$  vs. % (w/w)  $\text{H}_2\text{SO}_4$ . Vertical bars represent uncertainties.

where  $B$  is the normalized area of the band in the sulfuric acid solution considered,  $A$  is the respective area in Table 3 or 4 and  $A_{\text{max}}$  is the maximum value of  $A$  for the band studied (see Table 2). The normalization (Eq. 4) was used in order to give equal weights for all species in regression analysis. The respective examples are shown in Figs 4—6. For a given aqueous sulfuric acid solution with a molar concentration  $C_T$  we can write a balance equation

$$C_T = C_{\text{SO}_4\text{AQ}} + C_{\text{SO}_4\text{IP}} + C_{\text{HSO}_4\text{AQ}} + C_{\text{HSO}_4\text{IP}} + C_{\text{H}_2\text{SO}_4} \quad (5)$$

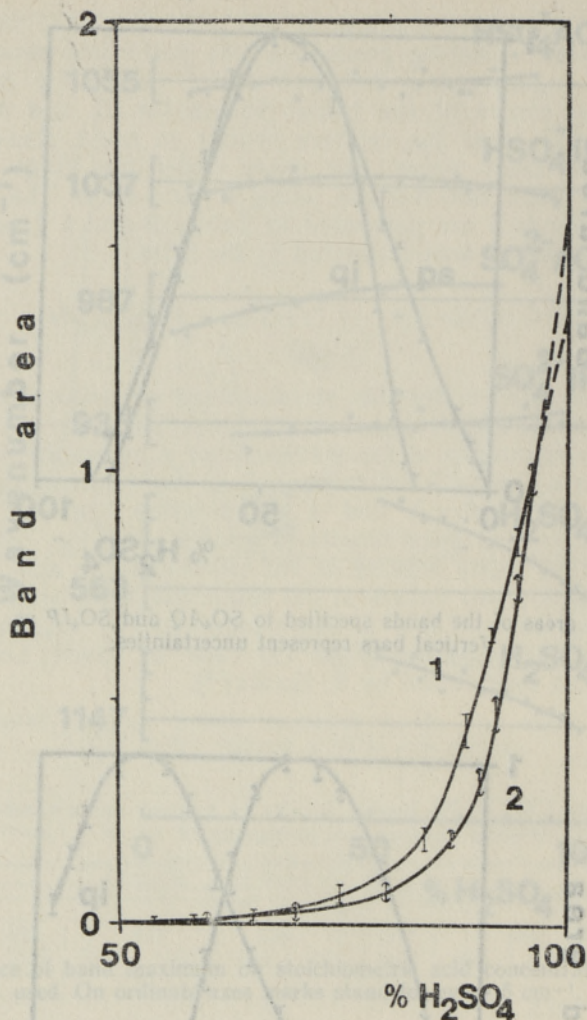


Fig. 6. Normalized areas of the bands specified to un-ionized sulfuric acid. 1 — at 563 cm<sup>-1</sup> and 2 — at 1147 cm<sup>-1</sup> vs. % (w/w) H<sub>2</sub>SO<sub>4</sub>. The dashed lines show the extrapolation to 100% H<sub>2</sub>SO<sub>4</sub>. Vertical bars represent uncertainties.

Table 5

Estimation of concentration for unionized sulfuric acid (mol/l)

| % H <sub>2</sub> SO <sub>4</sub> | 563 cm <sup>-1</sup> | 1147 cm <sup>-1</sup> | Average |
|----------------------------------|----------------------|-----------------------|---------|
| 54.40                            | 0                    | 0                     | 0       |
| 58.49                            | 0.14                 | 0.12                  | 0.13    |
| 59.88                            | 0.14                 | 0.12                  | 0.13    |
| 65.26                            | 0.27                 | 0.24                  | 0.26    |
| 67.72                            | 0.41                 | 0.24                  | 0.33    |
| 69.96                            | 0.41                 | 0.36                  | 0.39    |
| 75.05                            | 0.82                 | 0.48                  | 0.65    |
| 80.10                            | 1.50                 | 0.84                  | 1.17    |
| 84.26                            | 2.60                 | 1.56                  | 2.08    |
| 87.42                            | 4.23                 | 2.52                  | 3.38    |
| 89.58                            | 7.10                 | 3.60                  | 5.35    |
| 90.63                            | 8.05                 | 4.32                  | 6.18    |
| 92.09                            | 9.42                 | 5.40                  | 7.41    |
| 94.29                            | 11.60                | 8.15                  | 9.88    |
| 96.71                            | 13.65                | 12.00                 | 12.83   |



Normalized band areas ( $B_i$ ) of species

| % H <sub>2</sub> SO <sub>4</sub> | SO <sub>4</sub> AQ | SO <sub>4</sub> IP | H <sub>2</sub> SO <sub>4</sub> AQ | HSO <sub>4</sub> IP | H <sub>2</sub> SO <sub>4</sub> * | H <sub>2</sub> SO <sub>4</sub> ** |
|----------------------------------|--------------------|--------------------|-----------------------------------|---------------------|----------------------------------|-----------------------------------|
| 4.57                             | 0.08               |                    | 0.15                              |                     |                                  |                                   |
| 8.05                             | 0.15               |                    | 0.28                              | 0.01                |                                  |                                   |
| 11.78                            | 0.25               |                    | 0.43                              | 0.03                |                                  |                                   |
| 15.86                            | 0.35               |                    | 0.55                              | 0.05                |                                  |                                   |
| 21.90                            | 0.51               | 0.19               | 0.74                              | 0.10                |                                  |                                   |
| 25.86                            | 0.60               | 0.37               | 0.83                              | 0.14                |                                  |                                   |
| 31.19                            | 0.72               | 0.67               | 0.91                              | 0.21                |                                  |                                   |
| 36.74                            | 0.85               | 0.89               | 0.99                              | 0.29                |                                  |                                   |
| 44.02                            | 0.96               | 0.98               | 1.00                              | 0.38                |                                  |                                   |
| 50.03                            | 1.00               | 1.00               | 0.95                              | 0.50                |                                  |                                   |
| 54.40                            | 0.99               | 0.96               | 0.80                              | 0.58                |                                  |                                   |
| 58.49                            | 0.92               | 0.87               | 0.65                              | 0.68                | 0.01                             | 0.01                              |
| 59.88                            | 0.87               | 0.82               | 0.56                              | 0.71                | 0.01                             | 0.01                              |
| 65.26                            | 0.71               | 0.67               | 0.35                              | 0.83                | 0.02                             | 0.02                              |
| 67.72                            | 0.62               | 0.59               | 0.25                              | 0.88                | 0.03                             | 0.02                              |
| 69.96                            | 0.56               | 0.52               | 0.19                              | 0.94                | 0.03                             | 0.03                              |
| 75.05                            | 0.37               | 0.37               | 0.11                              | 0.99                | 0.06                             | 0.04                              |
| 80.10                            | 0.10               | 0.22               | 0.04                              | 1.00                | 0.11                             | 0.07                              |
| 84.26                            |                    |                    |                                   | 0.97                | 0.19                             | 0.13                              |
| 87.42                            |                    |                    |                                   | 0.92                | 0.31                             | 0.21                              |
| 89.58                            |                    |                    |                                   | 0.85                | 0.52                             | 0.30                              |
| 90.63                            |                    |                    |                                   | 0.83                | 0.59                             | 0.36                              |
| 92.09                            |                    |                    |                                   | 0.79                | 0.69                             | 0.45                              |
| 94.29                            |                    |                    |                                   | 0.74                | 0.85                             | 0.68                              |
| 96.71                            |                    |                    |                                   | 0.62                | 1.00                             | 1.00                              |

\* Peak at 563 cm<sup>-1</sup>.\*\* Peak at 1147 cm<sup>-1</sup>.

The concentration of a species  $i$  ( $C_i$ ) can be expressed by (see also Eq. 3)

$$C_i = x_i B_i, \quad (6)$$

where  $B_i$  is the standardized band area (Eq. 4) and  $x_i$  is a constant because the observed band intensities were corrected by Eq. 1. In order to obtain the  $x_i$  value for un-ionized sulfuric acid ( $x_5$ ) we extrapolated the plot  $B_5$  vs. % acid up to 100% sulfuric acid (see Fig. 6) where  $C_5 = 18.61$  mole/L. The ratio  $x_5 = C_5/B_5$  yielded the  $x_5$  values for both the lines used (563 and 1147 cm<sup>-1</sup>). Un-ionized sulfuric acid concentrations ( $C_{H_2SO_4}$ ) calculated by Eq. 6 were averaged and are presented in Table 5. This enables us to obtain

$$C_T - C_{H_2SO_4} = \sum_{i=1}^4 x_i B_i, \quad (7)$$

where the species listed in Eq. 5 are denoted by  $i$ . Eq. 7 can be written for each of the 25 sulfuric acid solutions. This yields a set of 25 equations with 4 unknown coefficients ( $x_1, \dots, x_4$ ). Using the  $B_i$  values from Table 6 the following regression coefficients were obtained: SO<sub>4</sub>AQ,  $x_1 = -1.75 \pm 4.44$ , SO<sub>4</sub>IP,  $x_2 = -0.29 \pm 3.23$ , HSO<sub>4</sub>AQ,  $x_3 = 3.07 \pm 2.23$  and HSO<sub>4</sub>IP,  $x_4 = 12.60 \pm 0.66$  (the respective standard deviations at  $f=20$  are also presented). The negative values of  $x_1$  and  $x_2$  are meaningless and  $x_3$  is rather uncertain. This result is not unexpected because the scales  $B_1$ ,  $B_2$  and  $B_3$  are strongly correlated among themselves:  $R_{1,2} = 0.946$ ,  $R_{1,3} = 0.744$  and  $R_{2,3} = 0.595$ . The  $R_{1,2}$  value implies that there is no possibility of differentiating SO<sub>4</sub>AQ and SO<sub>4</sub>IP concentrations. In this situation the use of the equation

$$C_T - C_{H_2SO_4} - C_{SO_4^{2-}} = x_3 B_3 + x_4 B_4 \quad (8)$$

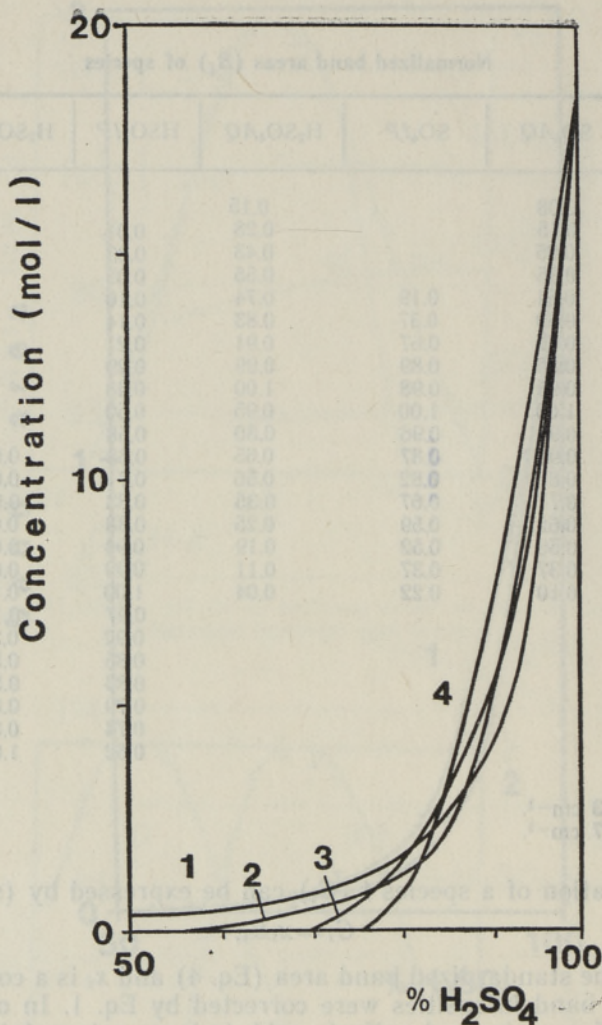


Fig. 7. Comparison of un-ionized sulfuric acid concentrations vs. % (w/w)  $H_2SO_4$  estimated by different authors. 1 — from [5], 2 — present study, 3 — from [3] and 4 — from [2].

is probably best we could do (where  $C_{SO_4^{2-}}$  is the total  $SO_4^{2-}$  concentration estimated by N. B. Librovich [2] or H. Chen [1]; see Fig. 8). Eq. 8 was applied to the data of 17 solutions (covering the range of 4.57–75.05%  $H_2SO_4$ ). Using the  $C_{SO_4^{2-}}$  values of N. B. Librovich [2] we obtained  $x_3 = 0.86 \pm 0.35$  and  $x_4 = 11.06 \pm 0.41$ . The respective results with H. Chen's data [1] were  $x_3 = 0.71 \pm 0.39$  and  $x_4 = 10.07 \pm 0.46$ . Assuming that the  $C_{SO_4^{2-}}$  values found by N. B. Librovich [2] and H. Chen [1] are probably the sum  $C_{SO_4AQ} + C_{SO_4IP}$  we used the equation

$$C_{SO_4^{2-}} = x_1 B_1 + x_2 B_2 \quad (9)$$

to obtain  $x_1$  and  $x_2$ . If  $C_{SO_4^{2-}}$  was taken from [2],  $x_1 = 0.92 \pm 0.18$ ,  $x_2 = 0.12 \pm 0.19$  and respectively, the data of H. Chen [1] yielded  $x_1 = 1.02 \pm 0.94$  and  $x_2 = 0.90 \pm 1.00$ .

The concentration profiles of  $SO_4AQ$ ,  $SO_4IP$ ,  $HSO_4AQ$ ,  $HSO_4IP$  and  $H_2SO_4$  estimated in this paper (Eq. 6) are presented in Table 7. A comparison of the data from Table 7 with the respective earlier ones (see

Table 7

## Concentrations of species (mol/l)

| $C_T$ | SO <sub>4</sub> AQ |      | SO <sub>4</sub> IP |      | HSO <sub>4</sub> AQ |      | HSO <sub>4</sub> IP |       | H <sub>2</sub> SO <sub>4</sub> |
|-------|--------------------|------|--------------------|------|---------------------|------|---------------------|-------|--------------------------------|
|       | [2]                | [1]  | [2]                | [1]  | 2                   | 1    | 2                   | 1     |                                |
| 0.478 | 0.07               | 0.08 |                    |      | 0.13                | 0.11 |                     |       |                                |
| 0.862 | 0.14               | 0.15 |                    |      | 0.24                | 0.20 | 0.11                | 0.10  |                                |
| 1.291 | 0.23               | 0.25 |                    |      | 0.37                | 0.30 | 0.33                | 0.30  |                                |
| 1.788 | 0.32               | 0.36 |                    |      | 0.47                | 0.39 | 0.55                | 0.50  |                                |
| 2.571 | 0.47               | 0.52 | 0.02               | 0.17 | 0.64                | 0.52 | 1.11                | 1.01  |                                |
| 3.116 | 0.55               | 0.61 | 0.05               | 0.33 | 0.72                | 0.59 | 1.55                | 1.41  |                                |
| 3.896 | 0.66               | 0.73 | 0.08               | 0.60 | 0.78                | 0.64 | 2.32                | 2.12  |                                |
| 4.761 | 0.78               | 0.87 | 0.11               | 0.80 | 0.85                | 0.70 | 3.21                | 2.92  |                                |
| 5.991 | 0.88               | 0.98 | 0.12               | 0.88 | 0.86                | 0.71 | 4.20                | 3.83  |                                |
| 7.098 | 0.92               | 1.02 | 0.12               | 0.90 | 0.82                | 0.67 | 5.53                | 5.04  |                                |
| 7.958 | 0.91               | 1.01 | 0.12               | 0.86 | 0.69                | 0.57 | 6.41                | 5.84  |                                |
| 8.813 | 0.84               | 0.94 | 0.11               | 0.78 | 0.56                | 0.46 | 7.52                | 6.85  | 0.13                           |
| 9.114 | 0.80               | 0.89 | 0.10               | 0.73 | 0.48                | 0.40 | 7.85                | 7.15  | 0.13                           |
| 10.32 | 0.65               | 0.72 | 0.08               | 0.60 | 0.30                | 0.25 | 9.18                | 8.36  | 0.26                           |
| 10.91 | 0.57               | 0.63 | 0.07               | 0.53 | 0.22                | 0.18 | 9.73                | 8.86  | 0.33                           |
| 11.45 | 0.51               | 0.57 | 0.06               | 0.47 | 0.16                | 0.13 | 10.40               | 9.47  | 0.39                           |
| 12.74 | 0.34               | 0.38 | 0.05               | 0.33 | 0.09                | 0.08 | 10.95               | 9.97  | 0.65                           |
| 14.07 | 0.09               | 0.10 | 0.03               | 0.20 |                     |      | 11.06               | 10.07 | 1.17                           |
| 15.17 |                    |      |                    |      |                     |      | 10.70               | 9.77  | 2.08                           |
| 15.93 |                    |      |                    |      |                     |      | 10.20               | 9.26  | 3.38                           |
| 16.50 |                    |      |                    |      |                     |      | 9.40                | 8.56  | 5.35                           |
| 16.75 |                    |      |                    |      |                     |      | 9.15                | 8.36  | 6.18                           |
| 17.08 |                    |      |                    |      |                     |      | 8.74                | 7.96  | 7.41                           |
| 17.56 |                    |      |                    |      |                     |      | 8.20                | 7.45  | 9.88                           |
| 18.05 |                    |      |                    |      |                     |      | 6.85                | 6.21  | 12.83                          |

1 — concentration of SO<sub>4</sub><sup>2-</sup> is from [1].

2 — concentration of SO<sub>4</sub><sup>2-</sup> is from [2].

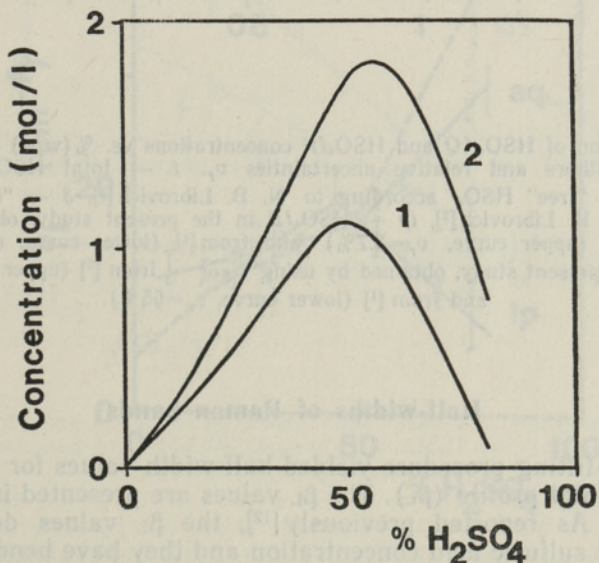


Fig. 8. Comparison of SO<sub>4</sub><sup>2-</sup> concentrations vs. % (w/w) H<sub>2</sub>SO<sub>4</sub> estimated by different authors. 1 — from [2], 2 — from [1].

Figs 7 and 9) leads to the following conclusions. First, the mean concentration profile for un-ionized sulfuric acid (see Fig. 7) agrees rather well with the earlier estimates [2, 3, 5]. Second, the results of H. Chen and D. E. Irish [1] are purely based on the relative integrated intensity of the band at  $981\text{ cm}^{-1}$  assigned to the sulfate ion. Their  $C_{\text{HSO}_4^-} = C_T - C_{\text{SO}_4^{2-}}$ . Therefore, disagreement with these concentration profiles [1] is not surprising. Third, the study of N. B. Librovich [2] is based on the unresolved bands and the concentration of  $\text{HSO}_4\text{IP}$  has been calculated as a difference  $C_T - (C_{\text{H}_2\text{SO}_4} + C_{\text{HSO}_4^-} + C_{\text{SO}_4^{2-}})$ . This results in large disagreement between species concentration profiles of his paper [2] and those of the present study (see Fig. 9).

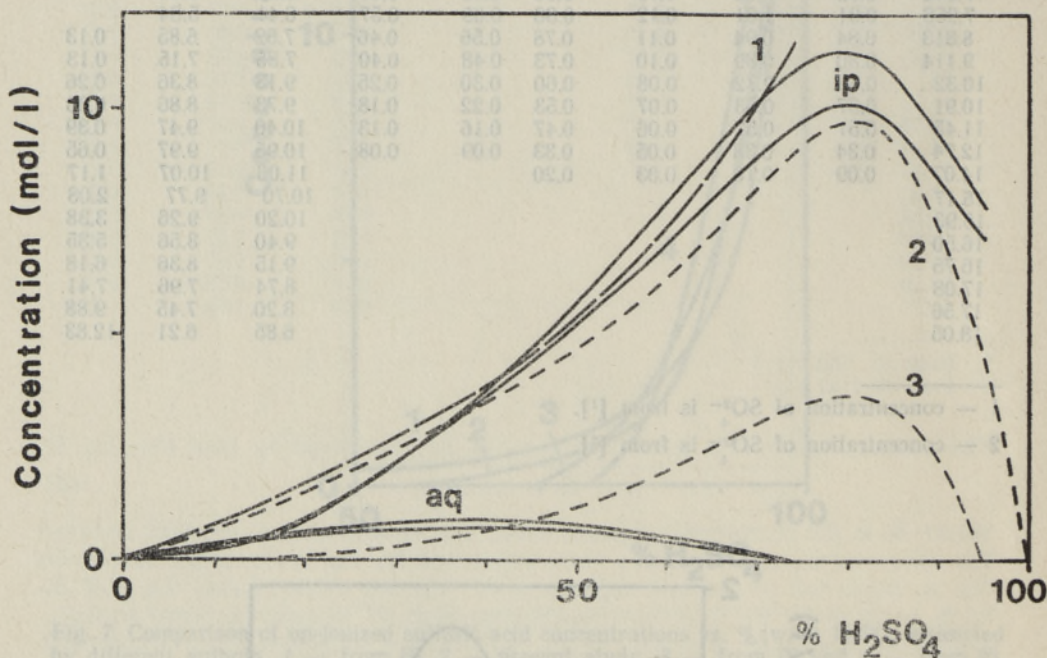


Fig. 9. Comparison of  $\text{HSO}_4\text{AQ}$  and  $\text{HSO}_4\text{IP}$  concentrations vs. % (w/w)  $\text{H}_2\text{SO}_4$  estimated by different authors and relative uncertainties  $v_r$ . 1 — total  $\text{HSO}_4$ , estimated by H. Chen [1], 2 — “free”  $\text{HSO}_4$  according to N. B. Librovich [2], 3 — “ionpaired”  $\text{HSO}_4$  according to N. B. Librovich [2], *ip* —  $\text{HSO}_4\text{IP}$  in the present study, obtained by using  $C_{\text{SO}_4^{2-}}$  from [2] (upper curve,  $v_r=3.7\%$ ) and from [1] (lower curve,  $v_r=4.6\%$ ), *aq* —  $\text{HSO}_4\text{AQ}$  in the present study, obtained by using  $C_{\text{SO}_4^{2-}}$  from [2] (upper curve,  $v_r=40\%$ ) and from [1] (lower curve,  $v_r=55\%$ ).

### Half-widths of Raman bands

The curve-fitting procedure yielded half-width values for the Lorentzian part of the Voigt profile ( $\beta_L$ ). The  $\beta_L$  values are presented in Table 8 and Figs 10—12. As reported previously [12], the  $\beta_L$  values depend on the stoichiometric sulfuric acid concentration and they have bends. In general, our data assure these findings but differ in details from those of S. Ikawa and M. Kimura [12]; see Figs 10 and 11. It should be pointed out that in two cases (for bands at  $935$  and  $1055\text{ cm}^{-1}$ ) our  $\beta_L$  values have maxima

Half-widths of Lorentzian component in Raman spectra ( $\text{cm}^{-1}$ )

| $\% \text{H}_2\text{SO}_4$ | $\text{SO}_4\text{AQ}$ | $\text{SO}_4\text{IP}$ | $\text{HSO}_4\text{AQ}$ | $\text{HSO}_4\text{IP}$ | $\text{H}_2\text{SO}_4$ |
|----------------------------|------------------------|------------------------|-------------------------|-------------------------|-------------------------|
| 4.57                       | 13.0                   |                        | 8.6                     | 12.0                    |                         |
| 8.05                       | 12.5                   |                        | 9.2                     | 13.2                    |                         |
| 11.78                      | 11.4                   |                        | 10.3                    | 15.2                    |                         |
| 15.86                      | 12.0                   |                        | 10.2                    | 16.0                    |                         |
| 21.90                      | 13.6                   | 13.0                   | 10.4                    | 14.0                    |                         |
| 25.86                      | 13.0                   | 16.1                   | 10.6                    | 14.8                    |                         |
| 31.19                      | 14.6                   | 15.2                   | 11.8                    | 19.6                    |                         |
| 36.74                      | 14.8                   | 17.0                   | 11.4                    | 19.4                    |                         |
| 44.02                      | 15.5                   | 17.1                   | 12.4                    | 18.5                    |                         |
| 50.02                      | 17.5                   | 21.0                   | 12.4                    | 21.6                    |                         |
| 54.40                      | 19.2                   | 19.5                   | 12.2                    | 20.4                    |                         |
| 58.49                      | 18.7                   | 16.0                   | 11.8                    | 20.4                    | 4.0                     |
| 59.88                      | 20.4                   | 13.2                   | 10.5                    | 20.6                    | 4.6                     |
| 65.26                      | 22.6                   | 11.0                   | 10.0                    | 21.4                    | 5.2                     |
| 67.72                      | 21.8                   | 12.0                   | 9.8                     | 22.3                    | 8.0                     |
| 69.96                      | 24.5                   | 11.4                   | 11.0                    | 24.1                    | 7.8                     |
| 75.05                      | 27.0                   | 12.0                   | 10.9                    | 23.6                    | 10.0                    |
| 80.10                      | 27.4                   | 7.1                    | 10.2                    | 23.9                    | 10.3                    |
| 84.26                      |                        |                        | 9.8                     | 24.0                    | 12.8                    |
| 87.42                      |                        |                        |                         | 26.0                    | 15.6                    |
| 89.58                      |                        |                        |                         | 27.2                    | 18.5                    |
| 90.63                      |                        |                        |                         | 26.3                    | 19.5                    |
| 92.09                      |                        |                        |                         | 27.4                    | 19.4                    |
| 94.29                      |                        |                        |                         | 27.4                    | 19.3                    |
| 96.71                      |                        |                        |                         | 24.8                    | 18.4                    |

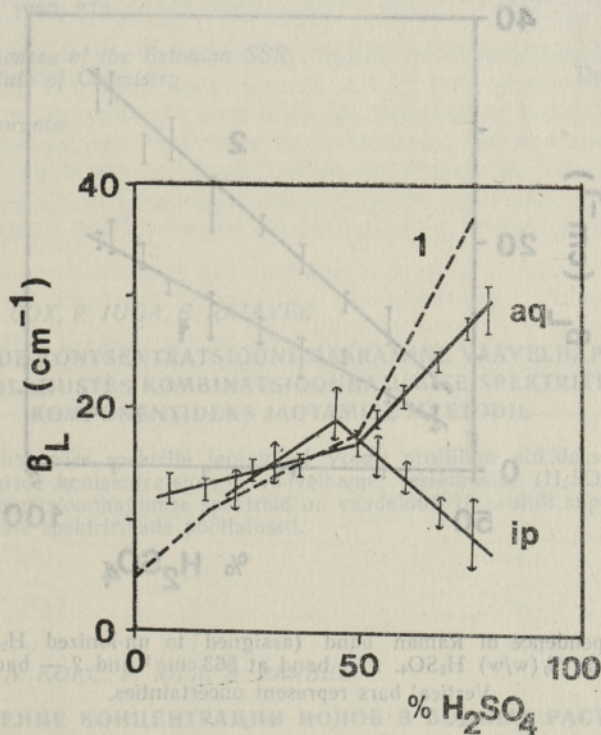


Fig. 10. The dependence of Raman band (assigned to sulfate ions) Lorentzian half-width ( $\beta_L$ ) on  $\% \text{H}_2\text{SO}_4$ . 1 — from [12], *aq* —  $\text{SO}_4\text{AQ}$  band at  $987 \text{ cm}^{-1}$  and *ip* —  $\text{SO}_4\text{IP}$  band at  $935 \text{ cm}^{-1}$ . Vertical bars represent uncertainties.

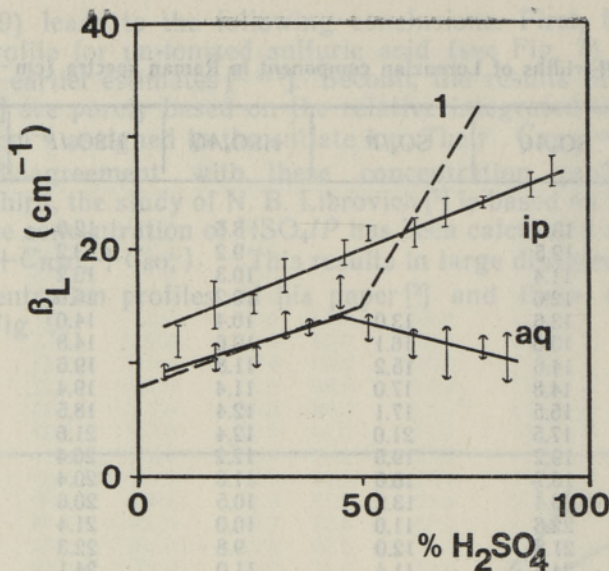


Fig. 11. The dependence of Raman band (assigned to bisulfate ions) Lorentzian half-width ( $\beta_L$ ) on % (w/w)  $H_2SO_4$ . 1 — from [12], *aq* —  $HSO_4AQ$  band at  $1055\text{ cm}^{-1}$  and *ip* —  $HSO_4IP$  band at  $1037\text{ cm}^{-1}$ . Vertical bars represent uncertainties.

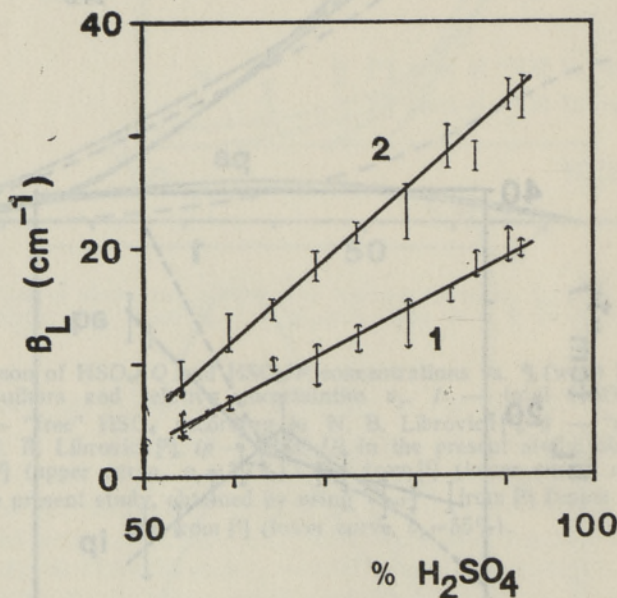


Fig. 12. The dependence of Raman band (assigned to un-ionized  $H_2SO_4$ ) Lorentzian half-width ( $\beta_L$ ) on % (w/w)  $H_2SO_4$ . 1 — band at  $563\text{ cm}^{-1}$  and 2 — band at  $1147\text{ cm}^{-1}$ . Vertical bars represent uncertainties.

at 45%  $H_2SO_4$  and bend down with increasing stoichiometric concentration. This indicates that the mean spectroscopic lifetimes of respective species ( $SO_4IP$  and  $HSO_4AQ$ ) pass through a minimum and increase if the stoichiometric acid concentration exceeds 45%.

## REFERENCES

1. *Chen, H., Irish, D. E.* A Raman spectral study of bisulfate sulfate system. II. Constitution, equilibria, and ultrafast proton transfer in sulfuric acid. — *J. Phys. Chem.*, 1971, **75**, 2072.
2. *Либрович Н. Б., Майоров В. Д.* Ионно-молекулярный состав водных растворов серной кислоты при 25°. — *Изв. АН СССР. Сер. хим.*, 1977, **51**, 684.
3. *Зарахани Н. Г., Маркин В. С., Залков Г. Е.* Гомогенные каталитические активные растворы. XII. Равновесный состав кислоты при 25°. — *Изв. АН СССР. Сер. хим.*, 1979, **53**, 2294.
4. *Cox, R. A., Yates, K.* Excess acidities. A generalized method for the determination of basicities in aqueous acid mixtures. — *J. Amer. Chem. Soc.*, 1978, **100**, 3861.
5. *Cox, R. A., Haldna, U. L., Idler, K. L., Yates, K.* Resolution of Raman spectra of aqueous sulfuric acid mixtures using principal factor analysis. — *Can. J. Chem.*, 1981, **59**, 2591.
6. *Malinowski, E. R., Cox, R. A., Haldna, U. L.* Factor analysis for isolation of the Raman spectra of aqueous sulfuric acid components. — *Anal. Chem.*, 1984, **56**, 778.
7. *Irish, D. E., Chen, H.* Equilibria and proton transfer in the bisulfate-sulfate system. — *J. Phys. Chem.*, 1970, **74**, 3796.
8. *Simonds, J. L.* Application of characteristic vector analysis to photographic optical response data. — *J. Opt. Soc. Amer.*, 1963, **53**, 968.
9. *Malinowski, E. R.* Obtaining the key set of typical vectors by factor analysis and subsequent isolation of component spectra. — *Anal. Chim. Acta*, 1982, **134**, 129.
10. *Irish, D. E., Chen, H.* The application of Raman spectroscopy to chemical analysis. — *Appl. Spectrosc.*, 1971, **25**, 1.
11. *Long, D. A.* Raman Spectroscopy. New York, 1977, 56.
12. *Ikawa, S., Kimura, M.* The study of the Raman band shape of sulfuric acid and proton transfer. — *Bull. Chem. Soc. Jap.*, 1976, **49**, 2051.
13. *Seshadri, J. S., Jones, R. N.* The shapes and intensities of infrared absorption bands. — *Spectrochim. Acta*, 1963, **19**, 1013.
14. *Kielkopf, J. F.* New approximation to the Voigt function with application to spectral line profile analysis. — *J. Opt. Soc. Amer.*, 1973, **63**, 987.
15. *Bevington, P. R.* Data Reduction and Error Analysis for the Physical Sciences. New York, 1969, 272.

Academy of Sciences of the Estonian SSR,  
Institute of Chemistry

Received  
Dec. 30, 1986

University of Toronto

Ü. HALDNA, R. A. COX, R. JUGA, E. RAJAVEE

### IOONIDE KONTSENTRATSIOONI MÄÄRAMINE VÄÄVELHAPPE VESILAHUSTES KOMBINATSIOONHAJUMISE SPEKTRITE KOMPONENTIDEKS JAOTAMISE MEETODIL

Kombinatsioonhajumise spektrite jaotamisel Voigti profiiliga piikideks on määratud ioonide ja ioonpaaride kontsentratsioonid väävelhappe vesilahustes ( $H_2SO_4$  massi % on 4,57—96,71). Kombinatsioonhajumise spektreid on vaadeldud 16 profiili superpositsioonina ja määratud osakeste spektriribade poollaiused.

Ю. ХАЛДНА, Р. А. КОКС, Р. ЮГА, Э. РАЯВЕЕ

### ОПРЕДЕЛЕНИЕ КОНЦЕНТРАЦИИ ИОНОВ В ВОДНЫХ РАСТВОРАХ СЕРНОЙ КИСЛОТЫ МЕТОДОМ РАЗДЕЛЕНИЯ КР-СПЕКТРОВ НА КОМПОНЕНТЫ

Путем разделения КР-спектров на профили Фойгта определены концентрации ионов и ионных пар в водных растворах серной кислоты в интервале 4,57—96,71% мас.  $H_2SO_4$ . КР-спектры рассмотрены в суперпозиции 16 отдельных полос. Для частиц определены значения ширин полос на полувысоте.